Reactive Sites in Isophorone Isomers: H/D-Exchange Studies and Quantum-Chemical Calculations

by **Eamonn F. Murphy**, **Thomas Bürgi**, and **Alfons Baiker***

Laboratorium für Technische Chemie, ETH, Hönggerberg, CH-8093 Zürich
(Phone: +41 1 6323153; fax: +41 1 6321163; e-mail: baiker@tech.chem.ethz.ch)

Dedicated to the memory of Professor *Luigi M. Venanzi*

Base-catalyzed H/D-exchange for α- and β-isophorone (**1** and **2**, resp.) was monitored by NMR spectroscopy to identify the number and nature of reactive sites. Results show that α-isophorone (**1**) undergoes H/D exchange at up to four different sites depending on reaction conditions. β-Isophorone (**2**), on the other hand, exhibits activity at two sites, predominantly at the α-position, under comparable conditions. Quantum-chemical calculations indicate that the thermodynamically more-stable anions formed upon proton abstraction from isophorone are not favored kinetically in all cases. Thermodynamically unfavorable H/D-exchange at the α-position in **1**, which is observed experimentally, is explained *via* intermediate formation of γ-isophorone (**3**) with subsequent conjugation to the α-isomer. Differences observed in the reactivities of the two isomers and differences in reactivity of **1** under various conditions in reactions involving proton abstraction as an initial step may be partly explained on the basis of these results.

1. Introduction. – Allylic oxidation of the readily available α- and β-isophorone isomers (α- and β-IP resp.; **1** and **2**, resp.) to ketoisophorone (KIP) **4** is an industrially important conversion providing a valuable intermediate for the flavor and fragrance industry [1][2]. Mild reaction conditions employed successfully for the oxidation of β-IP **2** have, however, proven entirely inappropriate for the more difficult oxidation of α-IP (**1**) [1]. In addition, competitive allylic oxidation at the β-methyl group in **1** affords mixtures of formylisophorone (FIP) **5** and KIP **4**, thereby compounding poor selectivity [1]. These differences in reactivity have been unexpected since it was suggested earlier that both isophorone isomers **1** and **2** share the same enolate intermediate formed *via* deprotonation under basic reaction conditions [3]. Recently, we have shown that phosphomolybdic acid in combination with DMSO and potassium *tert*-butoxide (K^tBuO) is an effective catalyst for the oxidation of α-IP **1** to KIP **4** under relatively mild conditions [4]. This system depended heavily on the solvent and base additive in order that high conversion with good selectivity to **4** be achieved simultaneously. Indeed, the above combination proved more effective than the previously investigated analogous solvent-free system for oxidation of **1** where N-bases were employed as additives [5].

To investigate these anomalies, we designed a series of NMR H/D-exchange experiments that emulate reaction conditions used in the successful β-IP oxidation with (salen)metal catalysts and our recent homogeneous system for α-IP oxidation [3][4]. In the past, it has been common practice to use rates of D-exchange to obtain information regarding relative C-acidities and carbanion stabilities [6][7]. In this work, experiments with deuterated methanol (CD_3OD) and deuterium oxide (D_2O) as deuterium sources for isophorone H/D-exchange have been studied by ^{1}H- and ^{13}C-NMR and COSY experiments.

In the present contribution, we concentrate on the influence of the solvent and base additive on the number of exchange sites and the relative rates of exchange in both isophorone isomers. The so-called *Brønsted* equation describing the relationship between kinetic and thermodynamic, or equilibrium, acidities has been established for various types of organic molecules [8][9]. Here, the kinetic acidities from H/D-exchange experiments are correlated with thermodynamic acidities as determined by quantum-chemical calculations for the three isomers α-, β-, and γ-IP **1** – **3**. Finally, these findings are used to rationalize the observed differences in reactivities of the two isomers **1** and **2** under comparable conditions in reactions that involve proton abstraction as a first step.

2. Results. – 2.1. *Assignment of Resonances and Identification of H/D-Exchange Sites in α- and β-Isophorones* (α- and β-IP, resp.; **1** *and* **2**, resp.) ^{1}H,^{1}H- and ^{1}H,^{13}C-NMR Correlation spectroscopy facilitated the unambiguous assignment of ^{1}H- and ^{13}C-NMR resonances, in particular protons at positions *B* and *C*, of both isomers **1** and **2** (*Fig. 1*). Observation of ^{1}H,D and ^{13}C,D coupling enabled identification of the reactive sites, and the degree of H/D-exchange at each site was then calculated from the respective resonance integrals. Under the conditions studied, H/D-exchange did not occur at position *E* of α- and β-IP **1** and **2**, respectively, even after 10 days, thereby allowing the corresponding integral to be used as a standard to measure the relative degree of exchange at other sites. In certain instances, for example, where Et_3N was used as additive, the *E*-proton resonance was buried under the Me signal of Et_3N. In this case, an alternative resonance was selected to calculate exchange rates as described below.

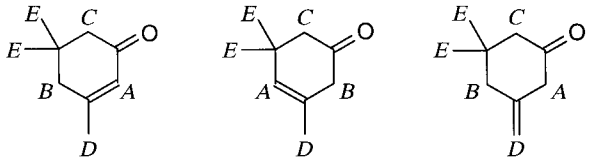

Fig. 1. *Labelling scheme used for protons at positions* A – E *in α-, β-, and γ-IP* **1** – **3**

2.2. *H/D-Exchange Under Conditions Effective for Homogeneous Oxidation of β-Isophorone* (β-IP; **2**) [3]. *Constantini et al.* described the oxidation of β-IP **2** to KIP **4** using homogeneous (salen)metal catalysts in solvents containing small amounts of H_2O and an organic base (*e.g.*, Et_3N) (*Scheme*) [3]. Bases investigated here for H/D-exchange experiments included Et_3N, trihexylamine, and pyridine, with CD_3OD as solvent and D-source. H/D-Exchange for α-IP **1**, which is not complicated by back-isomerization, was considered first. In Et_3N/CD_3OD solution, α-IP H/D-exchange was observed at four sites namely *D*, *C*, *A*, and *B*. The relative rates of H/D-exchange for *D*, *C*, and *A* of **1** are shown in *Fig. 2*. Exchange was relatively slow at *B* and was measurable only after extended periods (*ca.* 60 h). This point may be important considering previous oxidations of α-IP **1** where reaction times were typically greater than 100 h at elevated temperatures [1][5]. The absence of H/D-exchange at *B* was confirmed by ^{1}H (no ^{1}H,D coupling) and ^{13}C-NMR (no ^{13}C,D coupling) and allowed

the *B* integral to be used as a standard for experiments under 60 h duration. Substituting trihexylamine for Et_3N led to a drastic reduction in the rate of H/D-exchange (*Fig. 2*). With trihexylamine/CD_3OD, exchange at sites *B* and *C* of **1** was not observed up to 160 h. In alternative solvent/base systems, such as pyridine/$CDCl_3$/D_2O and pyridine/CD_3OD, H/D-exchange for α-IP **1** was not observed over an 8-day period.

Scheme. *Isomerization of* α*-IP* **1** *to* β*-IP* **2** *and* γ*-IP* **3**, *Oxidation of* **2** *to KIP* **4** *and of* **1** *to KIP/FIP Mixtures* **4**/**5** *with the Proposed Enolate Intermediates*

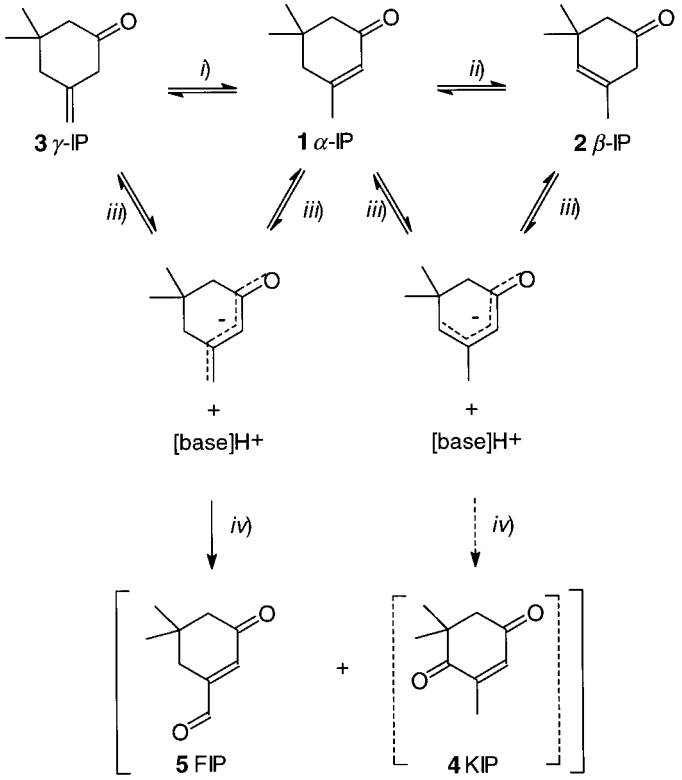

i) Photochemical reaction. *ii*) Typically acid-catalyzed at high temperature. *iii*) Amine catalyst. *iv*) Oxidant, usually air or dioxygen, in the presence of a homogeneous transition-metal catalyst.

Three processes were observed simultaneously during H/D-exchange studies with β-IP **2**; back-isomerization of **2** to α-IP **1**, H/D-exchange of **2**, and H/D-exchange of the back-isomerized **1**. Et_3N and trihexylamine both catalyzed the back-isomerization **2** → **1**. As shown in *Fig. 3*, Et_3N was more efficient than trihexylamine providing *ca.* 100% back-isomerization **2** → **1** at room temperature in just 18 h. In contrast to the tertiary amines, pyridine was significantly less effective for the isomerization **2** → **1** (7.4% of **1** after 2 days). In a control experiment in the absence of any N-base, a relatively low degree of back-isomerization (only 6.6% of **1** present in solution) was observed in CD_3OD after 8 days.

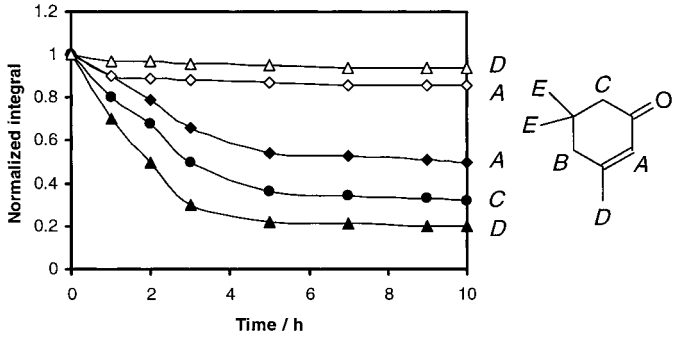

Fig. 2. *H/D-Exchange for α-IP* **1** *in* Et_3N/CD_3OD (◆, ●, ▲) *and in trihexylamine/*CD_3OD (◇, ○, △). Initial rate constants for H/D-exchange, calculated as described in the *Exper. Part*, were 0.441 and 0.177%/h for sites *D* and *A* in Et_3N, and 0.021 and 0.144%/h for sites *D* and *A* in trihexylamine.

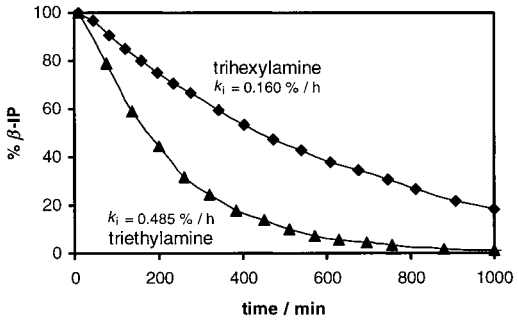

Fig. 3. *Back-isomerization of β-IP* **2** *to α-IP* **1** *in* Et_3N/CD_3OD (▲) *and trihexylamine/*CD_3OD (◆)

In agreement with the low rate of back-isomerization in CD_3OD in the absence of a base additive, H/D-exchange at all sites was slow for β-IP **2** under these conditions. In Et_3N/CD_3OD solution, H/D-exchange of **2** and the back-isomerized α-IP **1** were observed simultaneously. Exchange occurred only at positions *B* and *C* of **2**, with the former undergoing greater exchange under the time limit imposed by back-isomerization. D-Incorporation in the back-isomerized **1** was found at positions *A*, *C*, *D*, and also *B*, a consequence of back-isomerization, at very short reaction times. In contrast, H/D-exchange of **1** in Et_3N/CD_3OD under the same conditions was not observed at position *B* for reaction times under 60 h.

2.3. *H/D-Exchange under Conditions Effective for Homogeneous Catalytic Oxidation of α-Isophorone* (α-IP; **1**) [4]. Results for H/D-exchange of **1** in $(D_6)DMSO/D_2O$ are summarized in *Fig. 4*. H/D-Exchange was greatest at sites *A* and *D* with *ca.* 60% H/D-exchange in just 20 h, while *B* and *C* underwent relatively lower exchange in the same time interval (*ca.* 25%). Although results for the $(D_6)DMSO/D_2O$ and $(D_6)DMSO/D_2O/KO^tBu$ systems were identical after 20 h, the addition of KO^tBu to the solution gave rise to a significantly higher relative rate of H/D-exchange at sites *D* and *A* for shorter reaction times. The effect was more pronounced in the latter case with 24 *vs.* 11% H/D-exchange at site *A* after 1 h, with and without KO^tBu, respectively.

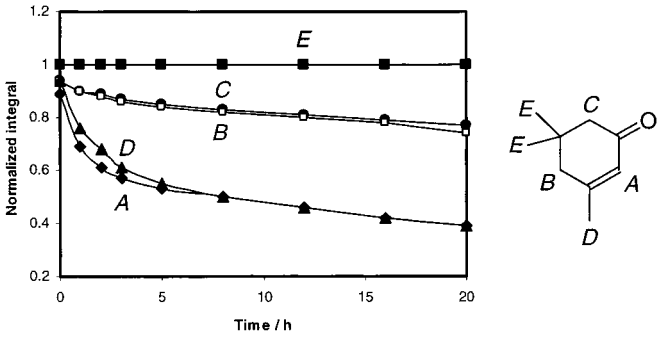

Fig. 4. *H/D-Exchange for α-IP* **1** *(D_6)DMSO/D_2O.* Initial rate constants for H/D-exchange, calculated as described in the *Exper. Part*, were 0.151, 0.172, and 0.021%/h for sites *D*, *A*, and *B*, respectively.

2.4. *Quantum-Chemical Calculations.* Relative stabilities of α-, β-, and γ-IP **1**–**3** are listed in *Table 1*. Optimized structures for α-IP **1** and β-IP **2** are depicted in *Fig. 5*; α-IP **1** is calculated to be more stable than β-IP **2** by 5.0 kcal/mol by means of the 6-31G(d,p) basis set. With the larger 6-311++G(d,p) basis set, the energy difference decreases to 4.6 kcal/mol. Incorporation of the solvent contribution for MeOH and DMSO in the calculation further reduces the energy difference between α- and β-IP (*Table 1*). In a sample of α-IP **1** at room temperature, the α/β-isomer ratio was 99.94, which corresponds to an equilibrium constant K of $5.7 \cdot 10^{-4}$ and a ΔG of 4.5 kcal/mol, in

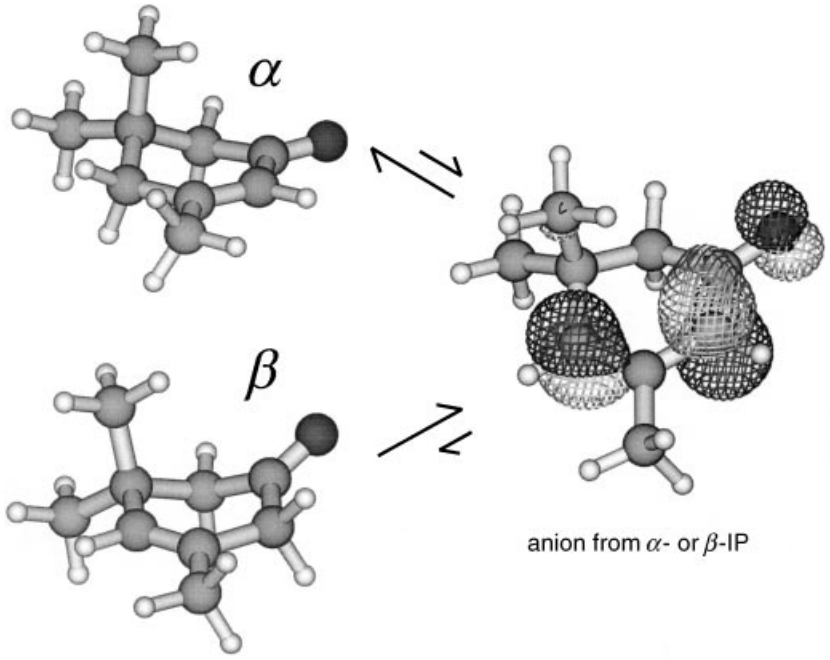

Fig. 5. *Optimized structures for α-IP* **1** *and β-IP* **2** *and the common anion formed on proton abstraction at sites* B *of* **1** *and* **2**. For the latter shared intermediate, the HOMO is also depicted.

Table 1. *Calculated Relative Energies* [kcal/mol] *of the Isophorone Isomers* **1**–**3**

	Basis Set			
	I[a])	II[b])	III[c]) (MeOH)	IV[d]) (DMSO)
α-IP **1**	0.0	0.0	0.0	0.0
β-IP **2**	5.0	4.6	3.4	4.1
γ-IP **3**	8.1	7.4	7.9	8.6

[a]) 6-31G(d,p). [b]) 6-311++G(d,p)//6-31G(d,p). [c]) 6-311++G(d,p)//6-31G(d,p) in MeOH. [d]) 6-311++G(d,p)//6-31G(d,p) in DMSO.

reasonable agreement with the calculation [10]. Similarly, for cyclohex-3-enone and cyclopent-3-enone, the equilibrium also rested heavily toward the conjugated isomer [11][12]; γ-IP **3** is *ca.* 8 kcal/mol less stable than the α-isomer **1**.

The calculated relative stabilities of the carbanions resulting on proton abstraction from α-, β-, and γ-IP **1**–**3** at the various C-atoms are given in *Table 2*. The calculated stabilities show the following trends: Incorporation of diffuse basis functions leads to a general decrease in the relative-energy differences of 5–10%. Incorporation of the solvent contribution (MeOH and DMSO) influences the relative energies. The most significant effect is on the carbanion formed by proton abstraction at position *C* of α-IP **1**, which is stabilized by more than 10 kcal/mol relative to carbanions formed on abstraction at *B* and *D*. A similar, less pronounced effect is also observed for the carbanion formed on abstraction at *C* of β-IP **3**, when the solvent contribution is considered.

Table 2. *Calculated Relative Energies* [kcal/mol] *of the Different Anions Generated on Proton Abstraction from* α-, β- *and* γ-*IP* **1**–**3** *at Sites* A–E

	α-IP **1** (basis set)				β-IP **2** (basis set)				γ-IP **3** (basis set)			
	I[a])	II[b])	III (MeOH)[c])	IV (DMSO)[d])	I[a])	II[b])	III (MeOH)[c])	IV (DMSO)[d])	I[a])	II[b])	III (MeOH)[c])	IV (DMSO)[d])
A	38.1	36.3	31.6	32.3	46.2	43.9	41.4	43.2	0.0[f])	0.0[f])	0.0[f])	0.0[f])
B	1.2[e])	1.3[e])	−1.1[e])	−1.1[e])	1.2[e])	1.3[e])	−1.1[e])	−1.1[e])	32.4[g])	30.6[g])	33.2[g])	33.8[g])
C	13.2	12.7	−1.4	−0.9	13.2	12.4	6.0	7.2	14.7	14.1	10.2	11.2
D	0.0[f])	0.0[f])	0.0[f])	0.0[f])	32.4[g])	30.6[g])	33.2[g])	33.8[g])	53.4	50.0	46.9	48.8
E	48.5	44.7	43.0	43.7	58.4	52.9	49.4	51.1	60.6	54.8	52.4	54.1

[a]) 6-31G(d,p). [b]) 6-311++G(d,p)//6-31G(d,p). [c]) 6-311++G(d,p)//6-31G(d,p) in MeOH. [d]) 6-311++G(d,p)//6-31G(d,p) in DMSO. [e]) Common anion of α- and β-IP. [f]) Common anion of α- and γ-IP. [g]) Common anion of β- and γ-IP.

For α-IP **1** the calculations predict a high relative probability for proton abstraction at positions *D*, *B*, and *C*. On the other hand, proton abstraction is unlikely at *A* and *E*. These predictions can be understood as follows on the basis of molecular-orbital arguments. Proton abstraction at positions *D* and *B* of **1** leads to an extended conjugated system accompanied by delocalization of the negative charge and hence stabilization of the anion. As shown in *Fig. 5* (right-hand side) for abstraction at site *B* the conjugated part of the molecule is flat for this carbanion. Furthermore, the O-atom, which can additionally stabilize the negative charge by an inductive electronic effect, is also part of the conjugated system. Abstraction at *C* leads to delocalization over three

atoms. The respective anion is considerably less stable in the gas phase compared to that generated by proton abstraction at *B* and *D*. Incorporation of the solvent contribution (MeOH, DMSO) in the calculation results in a large stabilization of the carbanions formed on abstraction at *C* with respect to *B* and *D*. In contrast, abstraction at *A* and *E* leads to high-energy carbanions with localized negative charge. In the case of β-IP **2**, abstraction at position *B* is most likely resulting in the carbanion shown in *Fig. 5*, followed by abstraction at *C*. Again, abstraction at *A* and *E* is unlikely. For γ-IP **2**, abstraction at position *A* is most likely, followed by abstraction at *C*, while abstraction at the other positions is again unlikely.

Proton abstraction at *B* of α-IP **1** leads to the same anion as abstraction at *B* of β-IP **2**. Similarly, other common anions are found between α- and γ-IP and β- and γ-IP. These anions can be thought of as intermediates in the isomerizations of α-, β-, and γ-IP (*Scheme*). The optimized structure for the common anion from α- and β-IP anion is depicted in *Fig. 5* (right-hand side). The most significant difference between carbanion stabilities of α- and β-IP is observed upon deprotonation at position *D*. For β-IP, abstraction at *D* is much less favorable compared to abstraction at the analogous position in α-IP, which can be attributed to reduced conjugation in the former carbanion.

The reactivities of the different C-sites of the carbanions toward an electrophile are related to their charge densities [13] and, in particular, to the highest occupied molecular orbital (HOMO). The HOMO for the common anion of α- and γ-IP is depicted in *Fig. 6*. It is evident, for example, that, on proton abstraction from α-IP **1** at *D*, an anion is generated with high probability of proton addition at position *A*, which would lead to γ-IP **3**. Similarly, on proton abstraction at *B* of α-IP **1** an anion is generated, which has high electron density at positions *A* and *B* (*Fig. 5*). Therefore, this anion is expected to have a relatively high probability to capture a proton at *A*, which leads to isomerization to β-IP **2**.

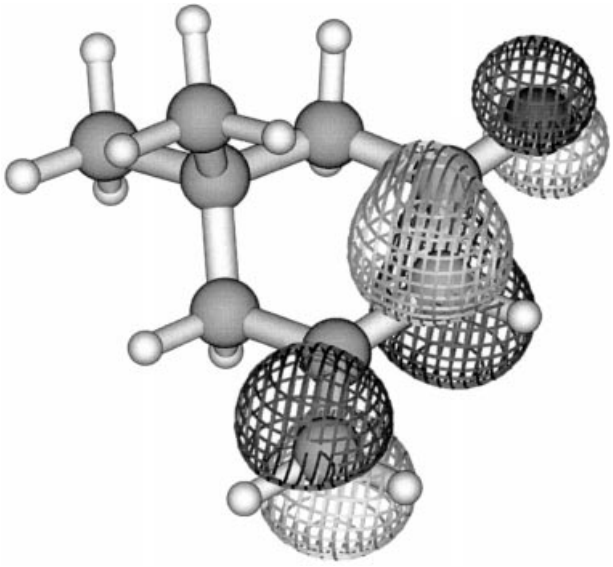

Fig. 6. *Optimized structure of the shared intermediate of* α*-IP* **1** *and* γ*-IP* **3**

3. Discussion. – Correlation of the kinetic and thermodynamic acidities for the two isophorone isomers **1** and **2** demonstrates the somewhat tenuous relationship that exists between the acidities as determined by the two methods [7][14a]. Et_3N-Catalyzed H/D-exchange of β-IP **2** and α-IP **1** in CD_3OD leads to H/D-exchange at two and four sites, respectively. Theoretical calculations for **2** predict that the most stable carbanion is formed by proton abstraction at position *B* and the second most stable by abstraction at *C*, in good agreement with the experimental findings. On the other hand, under the same conditions, two contradictions are found between experimental kinetic and calculated thermodynamic acidities for α-IP **1**. Thermodynamically, H/D-exchange is not expected at *A* of **1**, but is observed experimentally. This can be explained by invoking the intermediacy of γ-IP **3**. The latter is formed by proton abstraction at *D* followed by D-incorporation at the electron-rich site *A* of the anion (see *Fig. 6*). Attempts to find experimental evidence for the intermediacy of γ-IP **3** have been hindered by the likelihood that **3** readily back-isomerizes to α-IP **1** in the presence of base, retaining some D at position *A* of **1**. Previously, **3** has been prepared photochemically by deconjugation of **1** and was stable in solution at 0° for long periods [15][16]. Secondly, for N-bases, exchange at site *B* of **1** is not observed experimentally at < 60 h reaction time, but is predicted on the basis of thermodynamic calculations. One possible explanation is that proton abstraction at *B* is very fast, and due to steric hindrance by the three Me groups, solvent/base approach to coordinate the proton is prevented leading to an 'internal-return' effect [14b][17]. Alternatively, an inductive effect arising from the three electron-donating Me substituents leads to a build up of negative charge and destabilization at the reactive C-atom as it approaches the transition state. Of the two possible explanations, it is likely, given that the rate of H/D-exchange is almost independent of base type, that the latter kinetic control is responsible for the absence of H/D-exchange at position *B*.

The existence of common carbanions, which are generated on proton abstraction from different sites of the parent isophorone isomers, allows the relative thermodynamic acidities of these sites to be determined. For example, abstraction at position *D* of α-IP **1** leads to the same carbanion as abstraction at position *A* of γ-IP **3**. The fact that **3** is much less stable than **1** thus means that site *A* of **3** is much more acidic than site *D* of **1** and much faster proton exchange is, therefore, expected for the former.

The influence of base is significant in H/D-exchange experiments of **1**, essentially highlighting the unique role of Et_3N over trihexylamine and pyridine. In comparison with Et_3N, the bulky tertiary amine trihexylamine is less efficient for H/D-exchange, while the aromatic amine pyridine does not catalyze H/D-exchange. Similar steric effects have been observed previously for bulky tertiary amines [12]. In (D_6)DMSO/D_2O, the addition of KO^{t}Bu increases slightly the initial preference for exchange at *D* and *A* of **1** compared to the neat solvent. In conjugation experiments, neutral bases such as tertiary amines are known to be *ca.* 100-fold more effective catalysts than negatively charged bases (*e.g.*, butoxides, phosphates) [12][13]. Similarly, the greater efficiency of tertiary amines relative to oxobases in isophorone H/D-exchange can be attributed to an electrostatic effect. In the transition-state for proton removal, a favorable electrostatic interaction exists between the partial negative charge on the isophorone and the partial positive charge on the amine catalyst. In the case of (D_6)DMSO/D_2O/KO^{t}Bu, both the substrate and the base catalyst have some negative

charge in the corresponding transition state. These electrostatic interactions are unfavorable in the latter case and may be responsible for the lower rates of H/D-exchange catalyzed by (D_6)DMSO/D_2O/KO^{t}Bu compared with Et_3N/CD_3OD.

The question arises as to how much of the observed acidity is caused by the solvent. For α-IP **1**, H/D-exchange in (D_6)DMSO is fast compared to exchange in CD_3OD in the absence of an amine catalyst. Such large differences are often observed, even in relative acidities, on changing the solvent from CD_3OD to (D_6)DMSO [18]. Incorporating (D_6)DMSO/D_2O/KO^{t}Bu clearly increases the preference for sites *A* and *D* compared to Et_3N/CD_3OD and increases the rate of exchange with respect to the trihexylamine experiment. This is attributed to the greater ability of (D_6)DMSO to solvate a proton, leading to increased acidity [18]. *Constantini et al.* reported that protic solvents such as alcohols (*e.g.* CD_3OD) catalyze the back-isomerization of β-IP **2** to α-IP **1** [3]. It is now evident that back-isomerization occurs predominantly in the presence of both a N-base and protic solvent, and depends strongly on the type of base. Ion-pairing is unlikely to play a role in this work since, at low concentrations, it is rarely observed in solvents with dielectric constants greater than 30 (ε(MeOH) 32.6 and ε(DMSO) 49.0) [14c][19]. In addition, highly delocalized carbanions, such as the allylic anions of isophorone, do not tend to form ion pairs even in solvents with low dielectric constant [14d][20]. It must be added, however, that intrinsic structural effects of the parent molecules free of solvent effects are available only *via* gas-phase acidity measurements [21].

Deconjugation of α- to β-IP is an industrially important process and has been studied in detail (*Scheme*) [22][23]. Isomerizations of β- and γ- to α-IP require proton transfer between two C-atoms and can formally be regarded as 1,3-shifts [13]. In conjugation studies of β-enones, protonation at C(α) is typically more rapid than at C(γ), and thus protonation at the latter site is assumed to be the rate-limiting step in the base-catalyzed conjugation [13]. Given that the rate of proton abstraction at position *B* of β-IP **2** to generate the allylic anion is fast, then the rate of back-isomerization depends on the relative rates of protonation at sites *A* (C(γ)) and *B* (C(α)) of the β-IP anion. α- and β-IP share a common anion in isomerization (*Fig. 5*), and the preponderance of the α-isomer at moderate temperatures can be related to the thermodynamic stability of this isomer, *i.e.* exchange at C(α) of the anion can be very fast and reversible, while exchange at C(γ) is possibly slower but irreversible since α-IP **1** is more stable. Back-isomerization of β-IP **2** is faster in Et_3N than in trihexylamine, suggesting that the three Me groups prevent approach of the sterically more bulky ammonium ion and substantiating that protonation at position *A* of the β-IP anion is rate-determining in the back-isomerization.

The aforementioned findings can provide some possible explanations for the very different reactivities of the isophorone isomers in processes involving proton abstraction, such as isomerization and oxidation. In the allylic oxidation of α-IP **1**, FIP **5**, which is formed by competitive allylic oxidation at site *D*, is often observed as the main by-product. On the other hand, **5** is not detected in oxidations of β-IP **2** to KIP **4**. It now appears likely that this is a consequence of the relatively high acidity at position *D* of **1** compared with the analogous position of β-IP **2**. As shown in the *Scheme*, deprotonation at *B* and *D* of α-IP **1** effectively affords two distinct reaction intermediates. Proton abstractions at these positions are the important first steps in

the catalytic isomerization and also in the oxidation that lead to mixtures of KIP **4** and FIP **5** under oxidizing conditions. In CD_3OD and in the presence of N-bases, H/D-exchange at *B* is only observed at very long reaction times, while in (D_6)DMSO, exchange at *B* is much faster. Relatively facile proton solvation by (D_6)DMSO at site *B* may, therefore, be the reason why KIP **4** is obtained in good selectivity in DMSO, even in the absence of a base additive. In the patent literature, attempts have been described to improve selectivity in the catalytic oxidation of **1** in which air instead of dioxygen is used as oxidant, and by running the reaction for longer times at higher temperatures [1]. This would appear to support our view that exchange at *B* leads to **4** since H/D-exchange in Et_3N/CD_3OD also becomes important at site *B* in **1** after longer periods. In general, the existence of a greater number of sites for deprotonation/protonation will lead to increased numbers of reaction pathways, deprotonation being the rate-determining step in isomerization and allylic oxidation under basic conditions. This may subsequently manifest itself as poor selectivity in the catalytic conversions of isophorone [1].

4. Conclusion. – By means of NMR spectroscopy and H/D-exchange experiments, differences in the reactivities of the isophorone isomers in solution were found under conditions typical for catalytic isomerization and allylic oxidation. A combination of quantum-chemical calculations and the H/D-exchange results may be used to rationalize the dissimilar behaviors of the two isomers **1** and **2**. This work demonstrates that, on progressing to larger cyclic olefins, the difficulty in achieving high selectivity in such reactions may be attributed in part to the variety and number of sites for proton abstraction that pervade. Achieving high selectivity, therefore, ultimately places high demands on catalyst design and a judicious choice of reaction conditions.

The authors are grateful for grants of computer time at the ETH Zürich and *CSCS Manno*, and to *F. Hoffmann-La Roche Ltd*. and the ETH Zürich for financial support. Mr. *Felix Bangerter* is kindly acknowledged for recording NMR spectra and Dr. *Michael Schneider* for useful discussion.

Experimental Part

Materials. α-IP **1** and β-IP **2** were supplied by *F. Hoffmann-La Roche Ltd*. Deuterated solvents CD_3OD, D_2O, (D_6)DMSO, and $CDCl_3$ were purchased from *Aldrich*. Bases including pyridine, Et_3N, trihexylamine, and KO^{t}Bu were used as supplied by *Fluka*.

^{1}H- and ^{13}C-NMR Spectra. They were recorded at 300 K with a *Bruker* 300-MHz spectrometer. In a typical experiment with N-base additive, amine (0.018 mmol) was added to a soln. of isophorone (0.025 g, 0.18 mmol) and CD_3OD (0.60 ml). The time of mixing was set at 0 h. In experiments with (D_6)DMSO as solvent, α-IP **1** (0.025 g, 0.18 mmol) was mixed in (D_6)DMSO (0.60 ml), and D_2O (0.10 ml, *ca.* 6 mmol) was added at time 0 h. The same procedure was repeated with a mixture of **1** (0.025 g, 0.18 mmol) and KO^{t}Bu (0.002 g, 0.018 mmol). The spectra were then recorded at the time intervals described in the *Figs.* The integrals measured correspond to signals for 6 H–*E*, 3 H–*D*, 2 H–*C*, 2 H–*B*, and H–*A*. The rate of exchange of one proton at each site is described here and, therefore, the integrals have been normalized to compensate for the different weighting factors.

H/D Exchange Rates. They were calculated from the initial data points of the NMR experiments. The data were fitted to a first-order exponential by a *Levenberg-Marquardt* algorithm, which was used to calculate the initial rates. The given error is deduced from the fit of the data points to the exponential.

Theoretical Calculations. They were performed by density-functional theory with the hybrid density functional method B3LYP [24]. All structures were completely optimized with a 6-31G(d,p) basis set. For the anions, the optimized neutral parent compounds α-, β-, or γ-IP **1**–**3** after removal of a proton were selected as

the starting geometry for the optimization. At the minimum-energy structures, single point calculations were performed with a 6-311++G(d,p) basis set. The effect of the solvent was calculated with a polarizable continuum model (CPCM) [25] as implemented in Gaussian98 [26].

REFERENCES

[1] E. F. Murphy, T. Mallat, A. Baiker, *Catal. Today* **2000**, *57*, 115.
[2] O. Isler, in 'Carotenoids', Birkhäuser, Basel, 1971; P. Weyerstahl, T. Meisel, K. Mewes, S. Negahdari, *Liebigs Ann. Chem*. **1991**, 19; M. Shibagaki, S. Shibata, H. Kaneko, *Agric. Biol. Chem*. **1981**, *45*, 2911; J. N. Marx, *Tetrahedron* **1975**, *31*, 1251; E. Demole, P. Enggist, *Helv. Chim. Acta* **1974**, *57*, 2087.
[3] M. Constantini, A. Dromard, M. Jouffret, B. Brossard, J. Varagnat, *J. Mol. Catal.* **1980**, *7*, 89.
[4] E. F. Murphy, M. Schneider, T. Mallat, A. Baiker, *Synthesis* **2001**, *4*, 547.
[5] E. Widmer, M. Seuret, U.S. Pat. 3960966 (*Chem. Abstr*. **1976**, *84*, 164269).
[6] F. G. Bordwell, W. J. Boyle, J. A. Hautala, K. C. Yee, *J. Am. Chem. Soc*. **1969**, *91*, 4002.
[7] F. G. Bordwell, W. S. Matthews, N. R. Vanier, *J. Am. Chem. Soc.* **1975**, *97*, 442.
[8] A. Streitwieser, J. H. Hammons, *Progr. Phys. Org. Chem*. **1965**, *3*, 41.
[9] R. P. Bell, in 'The Proton in Chemistry', Cornell, Ithaca, New York, 1963.
[10] E. F. Murphy, T. Mallat, A. Baiker, M. Schneider, *Appl. Catal., A* **2000**, *197*, 295.
[11] N. Heap, G. H. Whitman, *J. Chem. Soc. B* **1966**, 164.
[12] D. L. Whalen, J. F. Weimaster, A. M. Ross, R. Radhe, *J. Am. Chem. Soc*. **1976**, *98*, 7319.
[13] R. M. Pollack, P. L. Bounds, C. L. Bevins, in 'The Chemistry of Enones', Eds. S. Patai, Z. Rappoport, Wiley, New York, 1989, Part 1, p. 559.
[14] C. D. Ritchie, in 'Physical Organic Chemistry, The Fundamental Concepts', 2nd edn. Marcel Dekker, New York, 1990; a) p. 48; b) p. 127; c) p. 211; d) p. 212.
[15] J. D. Shiloff, N. R. Hunter, *Can. J. Chem*. **1979**, *57*, 3301.
[16] A. Rudolph, A. C. Weedon, *J. Am. Chem. Soc*. **1989**, *111*, 8756.
[17] A. Schriesheim, C. A. Rowe Jr., L. Naslund, *J. Am. Chem. Soc*. **1963**, *85*, 2111.
[18] F. G. Bordwell, *Acc. Chem. Res.* **1988**, *21*, 456.
[19] A. J. Gordon, R. A. Ford, in 'The Chemist's Companion, A Handbook of Practical Data, Techniques and References', Wiley, New York, 1972.
[20] J. Lagowski, *Pure Appl. Chem*. **1971**, *25*, 429.
[21] R. W. Taft, F. G. Bordwell, *Acc. Chem. Res.* **1988**, *21*, 463.
[22] E. Widmer, U.S. Pat. 4005145 (*Chem. Abstr*. **1977**, *86*, 155268).
[23] P. Nösberger, A. J. Vieth, Eur. Pat. 488045 (*Chem. Abstr*. **1991**, *117*, 151177).
[24] A. D. Becke, *J. Chem. Phys.* **1993**, *98*, 5648.
[25] V. Barone, M. Cossi, J. Tomasi, *J. Comput. Chem*. **1998**, *19*, 404.
[26] M. J. Frisch, G. W. Trucks, H. B. Schlegel, G. E. Scuseria, M. A. Robb, J. R. Cheeseman, V. G. Zakrzewski, J. A. Montgomery, R. E. Stratmann, J. C. Burant, S. Dapprich, J. M. Millam, A. D. Daniels, K. N. Kudin, M. C. Strain, O. Farkas, J. Tomasi, V. Barone, M. Cossi, R. Cammi, B. Mennucci, C. Pomelli, C. Adamo, S. Clifford, J. Ochterski, G. A. Petersson, P. Y. Ayala, Q. Cui, K. Morokuma, D. K. Malick, A. D. Rabuck, K. Raghavachari, J. B. Foresman, J. Cioslowski, J. V. Ortiz, A. G. Baboul, B. B. Stefanov, G. Liu, A. Liashenko, P. Piskorz, I. Komaromi, R. Gomperts, R. L. Martin, D. J. Fox, T. Keith, M. A. Al-Laham, C. Y. Peng, A. Nanayakkara, C. Gonzalez, M. Challacombe, P. M. W. Gill, B. Johnson, W. Chen, M. W. Wong, J. L. Andres, C. Gonzalez, M. Head-Gordon, E. S. Replogle, J. A. Pople, 'GAUSSIAN98', Revision A.7, Gaussian Inc., Pittsburgh, PA, 1998.

Received March 28, 2001